Regulation of synaptic inhibition by phospho-dependent binding of the AP2 complex to a YECL motif in the $GABA_A$ receptor γ2 subunit

Josef T. Kittler*†, Guojun Chen‡, Viktoria Kukhtina§, Ardeschir Vahedi-Faridi¶, Zhenglin Gu‡, Verena Tretter‖, Katharine R. Smith*, Kristina McAinsh, I. Lorena Arancibia-Carcamo**, Wolfram Saenger¶, Volker Haucke§, Zhen Yan‡, and Stephen J. Moss‖**

Departments of *Physiology and **Pharmacology, University College London, Gower Street, London WC1E 6BT, United Kingdom; ‡Department of Physiology and Biophysics, State University of New York at Buffalo, Buffalo, NY 14214; Institute of Chemistry and Biochemistry, Departments of §Membrane Biochemistry and ¶Crystallography, Freie Universität Berlin, Takustrasse 6, 14195 Berlin, Germany; and ‖Department of Neuroscience, University of Pennsylvania, Philadelphia, PA 19104

Edited by Pietro V. De Camilli, Yale University School of Medicine, New Haven, CT, and approved December 21, 2007 (received for review August 22, 2007)

The regulation of the number of γ2-subunit-containing $GABA_A$ receptors ($GABA_A$Rs) present at synapses is critical for correct synaptic inhibition and animal behavior. This regulation occurs, in part, by the controlled removal of receptors from the membrane in clathrin-coated vesicles, but it remains unclear how clathrin recruitment to surface γ2-subunit-containing $GABA_A$Rs is regulated. Here, we identify a γ2-subunit-specific Yxxϕ-type-binding motif for the clathrin adaptor protein, AP2, which is located within a site for γ2-subunit tyrosine phosphorylation. Blocking $GABA_A$R-AP2 interactions via this motif increases synaptic responses within minutes. Crystallographic and biochemical studies reveal that phosphorylation of the Yxxϕ motif inhibits AP2 binding, leading to increased surface receptor number. In addition, the crystal structure provides an explanation for the high affinity of this motif for AP2 and suggests that γ2-subunit-containing heteromeric $GABA_A$Rs may be internalized as dimers or multimers. These data define a mechanism for tyrosine kinase regulation of $GABA_A$R surface levels and synaptic inhibition.

endocytosis | phosphorylation | structure | synaptic transmission | tyrosine kinase

The $GABA_A$ receptor ($GABA_A$R), a ligand-gated ion channel, mediates the majority of fast inhibitory synaptic transmission in the mammalian CNS. Identifying the molecular mechanisms important for regulating these receptors is essential for our understanding of how synaptic inhibition and neuronal excitability are controlled. $GABA_A$Rs are pentameric heterooligomers assembled from seven subunit classes (α1–6, β1–3, γ1–3, δ, ε, π, and θ). It is generally assumed that the majority of $GABA_A$Rs in the brain are assembled from at least 2 α-, 2 β-, and 1 γ2-subunits (1). The $GABA_A$R γ2-subunit confers important pharmacological, functional, and membrane-trafficking properties to $GABA_A$Rs, including benzodiazepine sensitivity, the selective targeting of $GABA_A$Rs to inhibitory postsynaptic domains, and correct animal behavior (2, 3). The phosphorylation of tyrosine (Y) residues within the γ2-subunit intracellular domain (ICD) at Y^{365} and Y^{367} increases $GABA_A$R function. However, the mechanisms that underlie this regulation remain unclear (4, 5). Furthermore, it has recently been demonstrated that altered membrane trafficking of γ2-subunit-containing $GABA_A$Rs may underlie certain pathological conditions, such as the generation of pharmacoresistance and self-sustaining seizures in status epilepticus and the increased excitotoxicity in ischemia (6–8). Currently, little is known regarding the molecular mechanisms and protein interactions that underlie γ2-subunit-dependent regulation of receptor membrane trafficking under normal or pathological conditions.

A potential mechanism to regulate synaptic inhibition is to alter the number of surface and synaptic $GABA_A$Rs. This surface receptor number can be determined, in part, by receptor endocytosis and the interaction with the clathrin adaptor protein (AP2) complex (9, 10). The AP2 complex is composed of α-, β2-, μ2-, and σ2-adaptin-subunits. The AP2-dependent internalization of neurotransmitter receptors has been demonstrated to underlie alterations in synaptic strength and plasticity (10–18). We have previously shown that $GABA_A$R ICDs interact with AP2 via directly binding to the μ2-subunit of AP2 (9, 10). In the case of $GABA_A$R β-subunits, the interaction with μ2 occurs via an atypical μ2 interaction motif and is negatively regulated by the phosphorylation of serine residues within this motif (10). In contrast, the molecular mechanisms of $GABA_A$R γ-subunit binding to AP2 remain unknown.

In this study, we use biochemical, electrophysiological, and structural approaches to characterize a γ2-subunit-specific Yxxϕ-type motif responsible for the binding of the AP2 complex to the $GABA_A$R γ2-subunit. We demonstrate that the γ2-subunit ICD can interact directly with μ2–AP2 via a $Y^{365}GY^{367}ECL^{370}$ (Yxxϕ type) AP2-binding motif that mediates high-affinity phospho-dependent binding to μ2–AP2. Targeting the YECL–AP2 interaction site by using interfering peptides rapidly increases inhibitory synaptic responses. Simultaneously targeting the YECL–AP2 interaction site in conjunction with the previously identified β3-subunit-binding site results in an additive response. Furthermore, the crystal structure of the YGYECL motif in complex with μ2–AP2 provides an explanation for the particularly high affinity of the YGYECL motif for μ2–AP2 and intriguingly also suggests that γ2-subunit-containing heteromeric $GABA_A$Rs may be internalized as dimers or multimers.

Results

A Yxxϕ-Type μ2–AP2-Binding Motif Specific to the $GABA_A$R γ2-Subunit. Tyrosine (Yxxϕ) motifs target a variety of cargo proteins, including some ion channels for clathrin-mediated endocytosis via direct binding to a pocket within subdomain A of μ2–AP2 (11, 12, 18–20). Analysis of the amino acid sequence of the γ2-subunit ICD revealed the presence of a conserved

Author contributions: G.C., V.K. and A.V.-F. contributed equally to this work; J.T.K., W.S., V.H., Z.Y., and S.J.M. designed research; J.T.K., G.C., V.K., A.V.-F., Z.G., V.T., and K.R.S. performed research; K.M. and I.L.A.-C. contributed new reagents/analytic tools; J.T.K., G.C., V.K., A.V.-F., W.S., V.H., and Z.Y. analyzed data; and J.T.K., W.S., and V.H. wrote the paper.

The authors declare no conflict of interest.

This article is a PNAS Direct Submission.

Data deposition: The X-ray structural coordinates have been deposited in the Protein Data Bank, www.pdb.org (PDB code 2PR9 and RCSB ID RCSB042702).

†To whom correspondence should be addressed. E-mail: j.kittler@ucl.ac.uk.

This article contains supporting information online at www.pnas.org/cgi/content/full/0707920105/DC1.

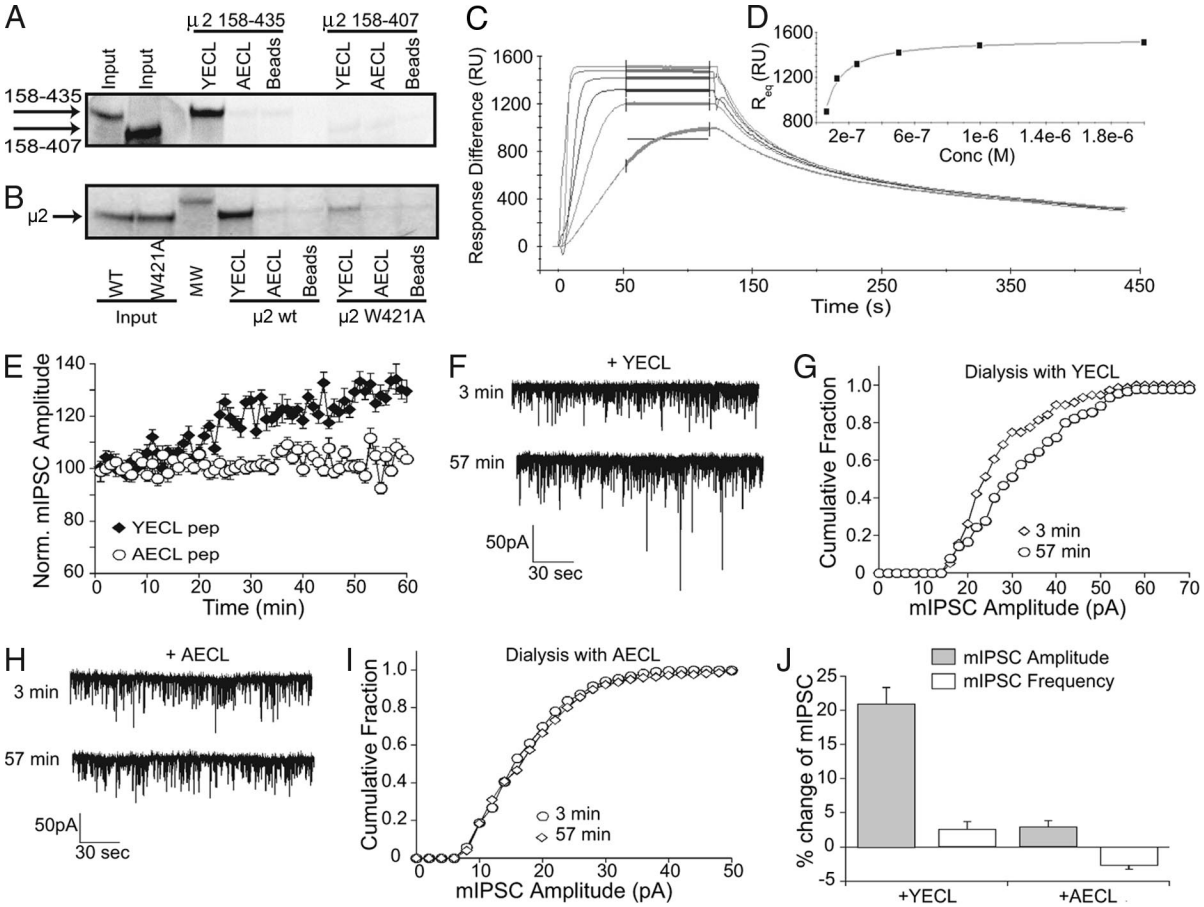

Fig. 1. Characterization of the YECL motif in $GABA_AR$ γ2-subunits that binds AP2. (*A*) YECL-pep, but not AECL-pep, interacts directly with [^{35}S]-labeled μ2–AP2 (residues 158–435 containing the Yxxϕ motif C-terminal-binding domain). A [^{35}S]-labeled truncated construct lacking the Yxxϕ motif-binding pocket (residues 158–407) no longer binds YECL-pep. (*B*) YECL, but not AECL, beads associate with purified bacterially expressed His-μ2 (residues 156–435). YECL beads show reduced association with an identical His-μ2 fusion protein containing W421 mutated to *A*. (*C* and *D*) SPR analysis of the binding of YECL-pep to purified His-μ2 reveals a K_d of 42.2 nM. (*C*) Sensograms of binding His-μ2 to YECL-pep performed on a BIACORE 2000. His-μ2 was injected at concentrations from 62 nM to 2 μM (lower to upper curves) over immobilized YECL-pep. The change in SPR signal during association and dissociation is shown in colored curves. Black bars are report points set on the sensograms in the steady-state region of the curve. (*D*) Plot of steady-state binding levels (R_{eq}) against concentrations of μ2 and fit to steady-state affinity model. (*E–J*) Functional consequences of blocking γ2-subunit interaction with AP2 on inhibitory synaptic responses. (*E*) Plot of normalized mIPSC amplitude as a function of time in cells dialyzed with YECL-pep and control AECL-pep. YECL-pep increases mIPSC amplitude. (*F* and *G*) Representative traces (*F*) and cumulative plots (G) from the 3rd and 57th minutes in cells dialysed with YECL-pep. (*H* and *I*) Representative traces (*H*) and cumulative plots (*I*) from the 3rd and 57th minutes in cells dialysed with control AECL-pep. (*J*) Bar plot summary showing the differential effects of YECL-pep and control AECL-pep on mIPSC amplitude and frequency.

putative classical Yxxϕ motif (YECL; residues 367–370) absent in $GABA_AR$ β-subunits. Peptides containing the Yxxϕ motif from other membrane proteins can effectively bind μ2–AP2 *in vitro* (11, 12). To determine whether the $Y^{367}ECL^{370}$ motif in the γ2-subunit ICD can bind μ2–AP2 directly, we synthesized a peptide containing the YECL motif and upstream sequence (YECL-pep) and tested its ability to interact with [^{35}S]-labeled μ2–AP2. We immobilized either YECL-pep or a version of this peptide containing Y^{367} mutated to alanine (A^{367}ECL-pep; control mutant) and looked at binding to a [^{35}S]-labeled fragment of μ2–AP2 (residues 158–435). Whereas YECL-pep exhibited robust binding to μ2–AP2, virtually no binding could be detected for the AECL mutant peptide or beads alone (Fig. 1*A*). We also identified the domain of μ2–AP2 that mediates binding to the $GABA_AR$ γ2-subunit YECL motif. The removal of the carboxyl-terminal 30 amino acids of μ2–AP2 (or even the mutation of W421 to alanine) (21) is sufficient to disrupt the binding of Yxxϕ-type signals to μ2–AP2. A [^{35}S]-labeled carboxyl-terminal truncation of μ2–AP2 (residues 158–407) could not bind to YECL-pep (Fig. 1*A*). Similar results were obtained when we examined the ability of bacterially expressed His-μ2 to bind YECL-pep beads. His-μ2 exhibited significant binding only to YECL-pep, but not to AECL-pep or beads alone (Fig. 1*B*). Furthermore, His-μ2 containing a W421A mutation exhibited substantially reduced interaction with the YECL-pep beads (≈15–20% binding remained).

In addition, we used surface plasmon resonance (SPR) to measure the affinity of the YECL-pep μ2–AP2 interaction as described previously for several other μ2–AP2 interaction motifs (10, 17, 22). Either YECL-pep (wild type) or AECL-pep (mutant used for the reference) was immobilized on a CM5 sensor surface, and their ability to bind recombinant His-μ2 was recorded in real time by using an SPR-based biosensor. This approach revealed that YECL-pep bound with a high nanomolar affinity to AP2 (K_d = 42.2 nM) (Fig. 1*C* and *D*), providing compelling evidence that the γ2-subunit-specific YECL motif can mediate high-affinity μ2–AP2 binding.

A Peptide Including the YECL Motif Increases Inhibitory Synaptic Responses. To determine the functional consequences of altering the recruitment of AP2 to the $GABA_AR$ via the γ2-subunit-

NEUROSCIENCE

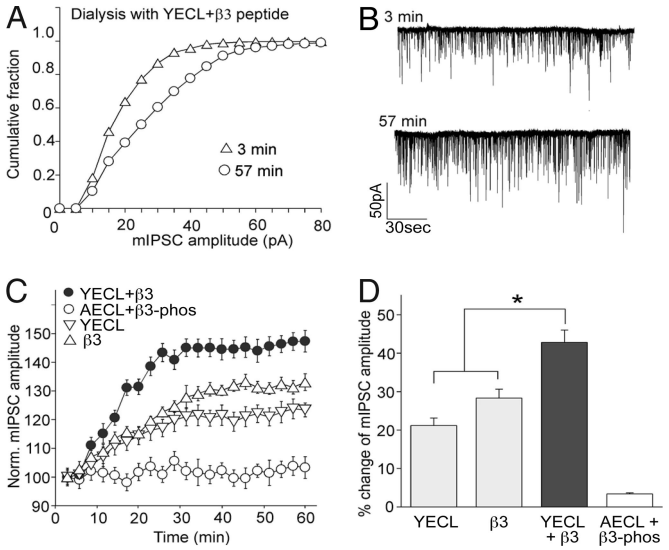

Fig. 2. Functional effects of simultaneously targeting the β3- and γ2-subunit interactions with μ2–AP2. (*A–D*) Effects of coinjecting β3-pep and YECL-pep on inhibitory synaptic responses. (*A* and *B*) Representative cumulative plots (*A*) and traces (*B*) from the 3rd and 57th minutes in cells codialysed with YECL-pep and β3-pep compared with control. (*C*) Plot of normalized mIPSC amplitude as a function of time in cells dialyzed with YECL-pep, β3-pep, YECL-pep plus β3-pep, or control AECL-pep plus β3-phos-pep. Codialysis of β3-pep and YECL-pep causes a marked increase in mIPSC amplitude over dialysis of either peptide alone. (*D*) Bar plot summary showing the differential effects on mIPSC amplitude of YECL-pep and β3-pep alone or codialysed together. Asterisk indicates significant difference from control ($P < 0.05$, $n = 6$).

specific YECL motif, we carried out whole-cell patch-clamp electrophysiological experiments to monitor the effects on inhibitory synaptic transmission of dialyzing a YECL motif-containing peptide [(YECL-pep) which we predicted would compete with AP2 binding and block receptor internalization] into neurons via the patch pipette. The control for these experiments was the identical peptide containing Y^{367} mutated to A (AECL-pep), which displays dramatically reduced AP2 binding and would therefore not compete with γ2-subunit-dependent AP2 binding to native receptors. As shown in Fig. 2, control striatal neurons showed a stable mIPSC amplitude within 60 min from the onset of recording (Fig. 1 *E* and *H–J*). In contrast, dialysis of the YECL-pep via the patch pipette caused a sustained increase in mIPSC amplitude (but not frequency) over the same 60-min time course (YECL-pep, 20.9 ± 2.4%, n = 7; control, 2.8 ± 0.9%, n = 7) (Fig. 1 *E–G* and *J*). Therefore, we conclude that the YECL μ2–AP2-binding motif within $GABA_AR$ γ-subunits plays a critical role in regulating the number of synaptic $GABA_ARs$ on a relatively rapid time scale. These results also correlate with an increase in the total number of surface $GABA_ARs$ in cultured neurons treated with a membrane-permeant YECL-pep, compared with control AECL-pep-treated neurons, as determined by using surface biotinylation [supporting information (SI) Fig. 6].

Simultaneous Targeting of $GABA_AR$ β3-Subunit and γ2-Subunit μ2–AP2 Interactions Causes an Additive Enhancement of mIPSCs. We have previously identified a major AP2-binding site in the $GABA_AR$ β3-subunit distinct from the YECL motif identified in γ2-subunits. Disruption of the β3–AP2 interaction [using a β3 AP2-binding motif peptide (β3-pep)] enhances the amplitude of mIPSCs in a similar fashion to what is seen here for dialysis of the YECL-pep (10), suggesting that both these μ2–AP2 interaction mechanisms are important for regulating the number of surface and synaptic $\alpha\beta\gamma$-containing $GABA_ARs$. To investigate this idea further, we monitored the consequences, on the size of mIPSCs, of simultaneously targeting both these AP2 interaction mechanisms with the $GABA_AR$ by using codialysis of β3-pep and YECL-pep. As shown in Fig. 2 *A–D*, codialysis of YECL-pep with the previously described β3-pep (10) over the same 60-min time course produced a significant additive effect on mIPSC amplitude, compared with interfering with $GABA_AR$–AP2 interactions individually by using β3-pep or YECL-pep alone or codialysed control peptides (β3-pep plus YECL-pep, 42.8 ± 3.2%, n = 6; β3-pep, 28.3 ± 2.3%, n = 6; YECL-pep, 21.2 ± 1.9%, n = 6; AECL plus β3-phos-pep, 3.4 ± 0.3%, n = 6). The control for β3-pep is an identical version of this peptide phosphorylated at two serine residues (β3-phos-pep) and that no longer interacts with AP2 (10).

Crystal Structure of the $GABA_AR$ γ2-Subunit-Derived YECL-Pep Complexed with μ2–AP2. To further examine the molecular nature of the interaction of the YECL motif and its surrounding residues with μ2–AP2, we cocrystallized a 10-aa peptide (DEEYGYECLD) corresponding to $GABA_AR$ γ2-subunit (residues 362–371) with the cargo-binding domain of μ2–AP2 (residues 157–435; μ2Δ157). The structure of the $GABA_AR$ YECL-pep complexed with μ2Δ157 was determined at a resolution of 2.5 Å (SI Table 1). Amino acid groups Glu2OE, Tyr6OH, Glu7O, N, and Leu9N of the YECL-pep interacted with μ2–AP2 (residues 157–435) amino acid groups Asp176OD, Lys203NZ, Lys319NZ, Lys420O, Val220O, N, Arg423NE, and NH1 as determined by electron density for peptide residues Asp-1 (D^{362}) to Asp-10 (D^{371}) (see Fig. 3 *A* and *B* and SI Table 2; for stereoview of μ2Δ157 complexed with YECL-pep, see SI Fig. 7), which encompasses the canonical tyrosine Yxxϕ endocytic signal ^{6}YECL^{9}. $GABA_AR$ YECL-pep binds at the identical surface location identified for the binding of the FYRALM and DYQRLN hexapeptides corresponding to the canonical Yxxϕ motifs of the EGF receptor (EGFR) and *trans*-Golgi network protein 38 (TGN-38), respectively (23), with Y^{367} and L^{370} sitting in chemically compatible pockets and playing key roles in mediating the interaction (Fig. 3*B*). Interestingly, the structure (Fig. 3 *A* and *B*) revealed additional interactions between μ2–AP2 and residues upstream of the canonical Y^{367} residue. Specifically, γ2-subunit residues D^{361}-Y^{365} (Asp-1, Glu-2, Glu-3, and Tyr-4) interact with residues Leu-316, Lys-319, Gln-318, Glu-391, Val-392, Pro-393, and Ile-425 of the μ2–AP2 subdomain A (Fig. 3 *A* and *B*). Similarly to Y^{367} (Tyr-6), a hydrophobic pocket is formed for Y^{365} (Tyr-4) (Fig. 3 *A* and *B*), with an additional salt bridge between Lys-319 and Glu-2 (see SI Tables 1 and 2). Therefore, our structural data reveal that, in addition to Y^{367} within the YECL motif, the upstream Y^{365} residue also plays a role as an additional specificity determinant of YECL-pep binding to μ2–AP2, similar to the three-pin plug mechanism reported for the association of a μ2–AP2 Yxxϕ-binding peptide derived from the membrane protein P-selectin (24).

Overall, 111 atomic contacts (2–5 Å) formed between μ2Δ157 and $GABA_AR$YECL-pep, compared with the 18 contacts formed by FYRALM (see SI Tables 1–4). A comparison of calculated contact surface areas for binding of YECL-pep and FYRALM-pep (CCP4 program ArealMol) shows an increase of 44% in contact surface area for $GABA_AR$YECL-pep [505 $Å^2$ (YECL) vs. 350 $Å^2$ (FYRALM)] (SI Fig. 8 and SI Table 4). The largest increase in contact areas is contributed by Leu-316, Gln-318, Lys-319, Glu-391, Val-392, Pro-393, and Ile-425 (Fig. 3*B*). Only His-416 shows a larger surface contact with FYRALM-pep. In the case of $GABA_AR$YECL-pep, His-416 has moved out of the binding pocket and no longer contributes to the van der Waals surface.

μ2–AP2 can form dimers, which could increase the strength and specificity of binding to dimeric receptors (23). Even larger differences are observed when the binding characteristics are

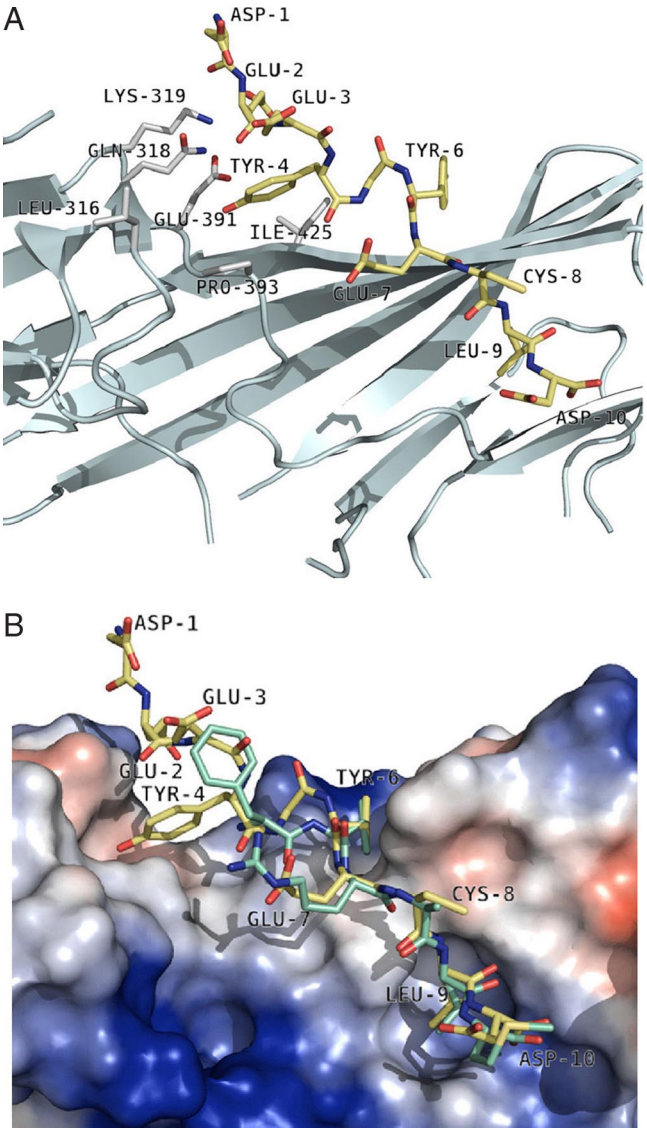

Fig. 3. Crystal structure of the $GABA_AR$ γ2-subunit YECL-pep complexed with μ2–AP2 (157–435). (*A*) Ribbon diagram showing the binding site within the signal-binding domain of μ2–AP2 complexed with a peptide corresponding to $GABA_AR$ γ2-subunit residues 362–371 (gold). (*B*) Surface representation of the γ2 peptide-binding interface with μ2–AP2, including an overlay with the endocytic motif of EGFR (turquoise) to compare binding of the two motifs.

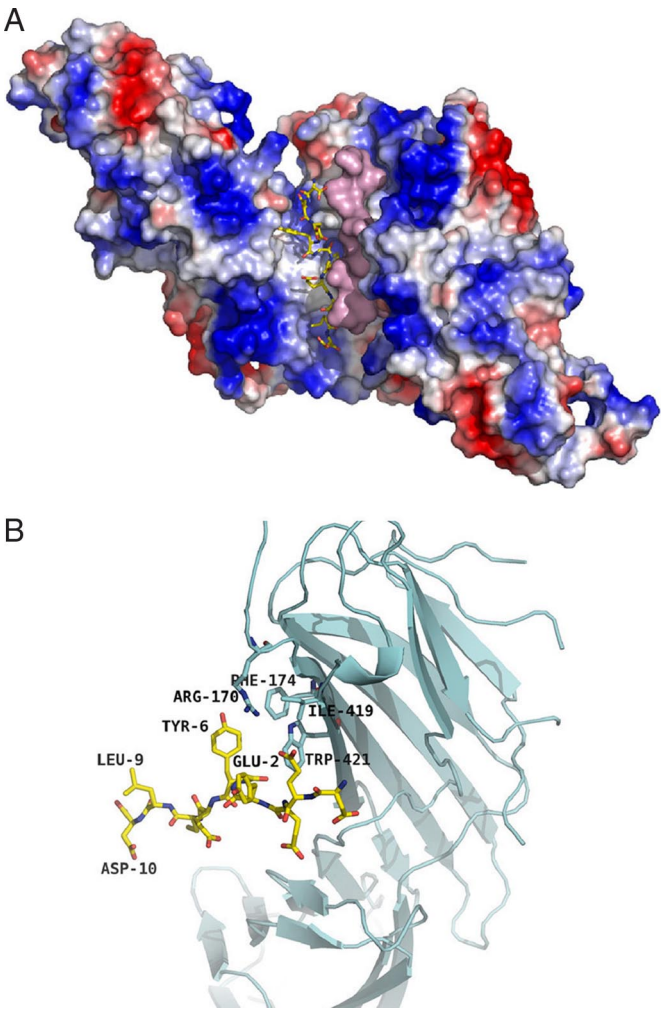

Fig. 4. Structure of the crystallographic dimer complexed with YECL-pep. (*A*) Structure of the crystallographic dimer showing the elongated banana-shaped binding pocket of a single YGYECL-pep on the μ2–AP2 dimer surface with the second peptide shown in surface representation. (*B*) Close-up view to show direct molecular interactions between the γ2-subunit YECL-pep and the other monomer in the crystallographic dimer.

compared for the peptide interactions with the $(\mu2\text{-YECL})_2$ dimer, the monomers being related by a crystallographic *C*2 axis (Fig. 4 *A* and *B* and SI Tables 3 and 5; for a stereoview of the crystallographic dimer complexed with YECL peptide, see SI Fig. 9). $GABA_AR$YECL-pep exhibits direct molecular interactions with residues Arg-170, Phe-174, Ile-419, and Trp-421 of the other monomer within the crystallographic dimer (see Fig. 4*B* and SI Table 3), which form additional binding pockets around the peptide residues Tyr-6 (Y^{367}) and Glu-2 (E^{368}). No such interactions exist in the case of the FYRALM–μ2 complex. Furthermore, the alignment of the two $GABA_AR$ YECL-pep dimers allows for the formation of one salt bridge (lys319NZ. . . Glu7OE) (SI Tables 2 and 3), which also is absent in the FYRALM–μ2 complex. Fig. 4*A* depicts the elongated binding pockets of $(\mu2\text{–AP2} \times \text{YECL-pep})_2$, one peptide shown as a wire model and the other in a surface representation. Importantly, these results suggest that γ2-subunit dimers (presumably with γ2-subunits contributed from two different heteromeric receptors) may be complexed within AP2-coated vesicles upon endocytosis, suggesting that multiple or possibly even clustered receptors may be internalized within one endocytic event.

μ2–AP2-Binding to the YECL Motif Is Regulated by Phosphorylation of Y^{365} and Y^{367}. Residues Y^{365} and Y^{367} within the γ2 subunit are major sites of tyrosine phosphorylation in the $GABA_AR$ and are substrates of SRC family tyrosine kinases both *in vitro* and *in vivo* (4, 5). The crystallographic data predict that phosphorylation at Y^{367} within the YGYECL motif would preclude μ2-binding because there is insufficient space to accommodate a phosphate group within the binding pocket (and, in addition, D^{473} within μ2–AP2 would repel binding), as has been shown previously for other tyrosine motif-AP2 interactions (11, 12, 23). In addition, the YECL peptide–μ2–AP2 structure reveals that, because Y^{365} also contributes to μ2–AP2 binding (by hydrogen bonding with E^{391}), phosphorylation at this site also may negatively regulate μ2–AP2 binding because phospho-Y^{365} would repel the interaction with E^{391}.

To test whether phosphorylation of Y^{365} and/or Y^{367} can indeed inhibit binding to μ2–AP2, we immobilized either the

NEUROSCIENCE

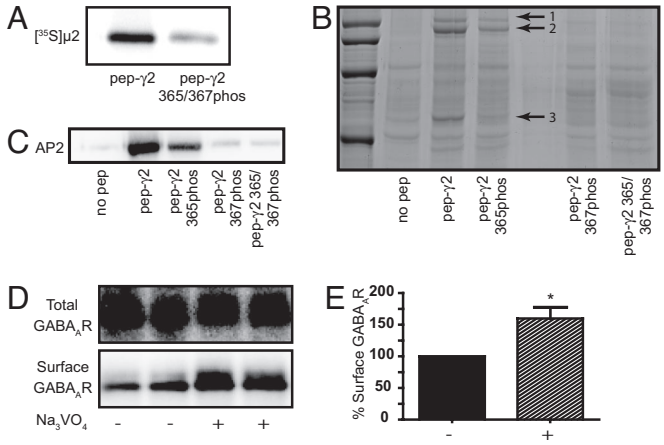

Fig. 5. Tyrosine phosphorylation inhibits interaction with AP2 and increases surface $GABA_AR$ number. (*A*) Inhibition of [^{35}S]-labeled μ2–AP2 binding to diphosphorylated (Y^{365} and Y^{367}) γ2 YECL-pep beads. (*B*) Copurification of AP2 subunits with YECL-pep beads from brain lysate as revealed by SDS/PAGE and Coomassie blue staining. Arrows show copurified AP2 subunits (identified after mass spectrometry of the highlighted bands, arrows 1–3, representing its AP2α1, AP2α2, and μ2–AP2, respectively). A clear reduction in AP2-associated bands can be seen for a peptide phosphorylated on Y^{365}, whereas phosphorylation of Y^{367} or Y^{365} and Y^{367} results in further reduction in binding. (*C*) Phosphorylation-dependent binding of YGYECL-pep to brain AP2 as revealed by Western blotting. (*D* and *E*) Cortical neurons were surface-biotinylated after treatment with orthovanadate to increase $GABA_AR$ phosphorylation at Y^{365} and Y^{367}. (*D*) Representative Western blot of one experiment showing a clear increase in surface receptor number upon orthovandate treatment. (*E*) Bar graph showing quantified cell-surface receptor levels with and without orthovanadate treatment. Asterisk indicates significant difference from control ($P < 0.05$, $n = 6$).

YECL-pep or a version of this peptide that had been chemically phosphorylated on Y^{365} and Y^{367} (YGYECL-phos) onto beads and looked at binding to [^{35}S]-labeled μ2–AP2. YECL-pep exhibited robust binding to μ2–AP2 in this assay (in agreement with the results using SPR), whereas a peptide that was chemically phosphorylated on both Y^{365} and Y^{367} bound virtually no [^{35}S]-labeled μ2–AP2 (Fig. 5*A*). We carried out similar experiments to test the binding of the tyrosine motif peptides in their phosphorylated or unphosphorylated forms to AP2 from brain lysate by using SDS/PAGE and detection of bound AP2 by either Coomassie blue staining followed by MALDI mass spectrometric analysis of bands from bound complexes or Western blotting with AP2 antibodies. When an unphosphorylated version of the peptide containing the YECL motif was coupled to beads and then exposed to brain lysate, Coomassie blue staining of bound protein complexes analyzed by SDS/PAGE revealed major interacting bands associated with this peptide at 50 and 115 kDa (these bands represent the correct molecular weight for the μ2- and α-subunits of AP2, respectively) (see Fig. 5*B*, lane 1). That these bands represented AP2 subunits was confirmed by the excision of the bands, followed by Maldi-TOF mass spectrometry, further confirming the ability of the YECL-pep to strongly interact with brain AP2. In contrast to the unphosphorylated peptide, binding of AP2 to a peptide phosphorylated on Y^{365} was reduced (as shown by much weaker Coomassie blue-stained bands at 50 and 115 kDa). A more substantial reduction in the interaction was observed when the peptide was phosphorylated on Y^{367}, whereas the greatest reduction was seen with the diphosphorylated peptide ($Y^{365phos}$ and $Y^{367phos}$), which showed essentially no AP2 binding (Fig. 5*B*). Similar results were obtained by Western blot analysis of YECL-pep brain pulldown assays by using an antibody to μ2–AP2 (Fig. 5*C*).

These results demonstrate that YGYECL motif binding to AP2 is regulated by phosphorylation and consequently predict that phosphorylation of Y^{365} and/or Y^{367} would block YGYECL-dependent, AP2-mediated internalization and result in an increase in surface receptor number (in agreement with earlier reports that SRC phosphorylation of Y^{365}/Y^{367} enhances receptor function) (4). It has been reported that in cortical neurons blocking tyrosine phosphatase activity by orthovanadate leads to a large increase in phosphorylation at Y^{365} and Y^{367} (5). To test whether treatment of cortical neurons with orthovanadate (increasing Y^{365}/Y^{367} phosphorylation) (5) also resulted in an increase in the number of surface $GABA_AR$ as would be predicted from the above results, we used surface biotinylation of cultured neurons, which, as we have previously shown, is an effective reporter of surface receptor number (25). Orthovanadate treatment produced a statistically significant increase of $159.7 \pm 11\%$ of control ($P < 0.05$, $n = 6$) in the cell-surface number of $GABA_ARs$ (Fig. 5 *D* and *E*). Together these results provide evidence that phosphorylation of Y^{365} and Y^{367} can directly regulate μ2–AP2-binding affinity and the number of surface $GABA_ARs$.

Discussion

Here, we reveal several key issues relating to the functional modulation of γ2-subunit-containing $GABA_ARs$. Using a combination of biochemical, crystallographic, and electrophysiological approaches, we demonstrate that a YECL motif in the γ2-subunit mediates interaction with the clathrin AP2 adaptor and that this YECL motif–AP2 interaction is important for the accumulation of synaptic $GABA_ARs$. The YECL motif interacts with the μ2–AP2 Yxxϕ motif-binding pocket, which is critically dependent on the C-terminal 28 residues in μ2–AP2, but independent of the basic patch interaction site in subdomain B of μ2 previously reported to interact with $GABA_AR$ β-subunits and AMPARs (10, 17). Cocrystallization of a decapeptide containing the γ2-subunit YECL motif with the signal-binding domain (residues 156–435) of μ2–AP2 revealed that the YECL motif binds in a similar manner to μ2–AP2 as to the canonical motifs from EGFR and TGN-38 (23), with Y^{367} and L^{370} sitting in chemically compatible pockets and playing key roles in mediating the interaction. Importantly, Y^{367} appears to be a major determinant of the interaction because binding is substantially lost upon mutagenesis of this residue to alanine. Moreover, it was apparent that several upstream residues (notably Y^{365}) act as additional specificity determinants of the interaction by binding into a third pocket on the μ2–AP2 protein surface formed by the aliphatic portions of Gln-318, Glu-391, and Pro-393. The additional interaction mediated by Y^{365} also may explain the high affinity of γ2-subunit Yxxϕ motif revealed by SPR (42.2 nM) (26) and is $\approx$8-fold higher than that previously reported by using SPR for the AP2-binding domain within the $GABA_AR$ β3-subunit (300 nM) (10).

It has been reported previously that μ2–AP2 can form dimers that could increase the strength and specificity of binding to dimeric receptors (23). Of significant interest, our current study demonstrates that the $GABA_AR$-derived YECL-pep forms van der Waals interactions with residues Arg-170, Phe-174, Ile-419, and Trp-421 of the μ2–AP2 crystallographic dimer. These residues provide additional binding pockets for the peptide residues Tyr-6 (Y^{367}) and Glu-2 (E^{363}). Furthermore, the alignment of the two $GABA_AR$ YECL-pep dimers allows for the formation of four electrostatic interactions. Because only one γ2-subunit is present per $GABA_AR$ heteromer, the γ2-subunit-containing receptors may be internalized as dimeric or multimeric clusters of receptors. In agreement with the possibility that heteromeric $GABA_ARs$ containing γ2-subunits may be able to dimerize and form clusters, it has been reported that the ICD of γ2-subunits can self-associate (27), which would allow two

YECL motifs to come together within a dimerized μ2–AP2 complex.

Dialysis of the YECL peptide (with a high affinity for AP2) into neurons significantly increased the amplitude of mIPSCs within tens of minutes, demonstrating that AP2 binding to γ2-subunits underlies the dynamic modulation of synaptic $GABA_AR$ number. Importantly, we demonstrate that the previously described β-subunit AP2-binding mechanism (10) and the γ2-subunit-specific YECL–AP2-binding mechanism described here can act either separately or together to modulate synaptic $GABA_AR$ number because simultaneously targeting both AP2 interaction mechanisms had a substantial additive effect on the inhibitory synaptic response. These results clearly demonstrate that synaptic $GABA_AR$ number can be controlled by at least two mechanisms for AP2-dependent receptor recruitment into the internalization pathway, one of which is γ2-subunit-selective.

There is accumulating evidence that the phosphorylation of $GABA_AR$ ICDs may regulate receptor cell-surface number (28). The crystal structure presented here reveals that phosphorylation of either Y^{365} and/or Y^{367} has a negative regulatory role on the binding affinity of AP2 to the YGYECL motif, which we confirm biochemically and which also has been suggested for other Yxxϕ-type interactions (23). Previous work showed that phosphorylation of Y^{365} and Y^{367} by the tyrosine kinase SRC both *in vitro* and *in vivo* enhances the receptor function in line with our current results (4, 5). We suggest that, in part, this functional enhancement may be due to phosphorylation at Y^{365} and Y^{367} inhibiting interaction with AP2, which we demonstrate here increases the number of surface (and potentially synaptic) $GABA_ARs$. Therefore, our work highlights a phospho-dependent mechanism to regulate $GABA_AR$ cell-surface levels and synaptic inhibition by tyrosine phosphorylation of γ2-subunits. Alterations in the phosphorylation state of Y^{365} and/or Y^{367} within the γ2-subunit during synaptic plasticity or in pathology may therefore underlie dynamic alterations in synaptic receptor number (6, 7, 29). Importantly, the insights presented here and the structural data within this study could pave the way for the development of acute chemical inhibitors that could be used to selectively block pathological γ2-subunit-dependent receptor internalization.

We have previously shown that phosphorylation at conserved serine residues (S408 and S409) in the $GABA_AR$ β3-subunits also can act as a molecular switch to regulate μ2–AP2 recruitment and the number of $GABA_ARs$ at inhibitory synapses (10, 30). The reason for two separate phospho-dependent μ2–AP2-binding mechanisms in the β- and γ-subunits is not clear, but the fact that the $GABA_AR$ β3-subunit and γ2-subunit AP2-binding motifs are regulated by different kinase families (i.e., serine/threonine or tyrosine kinase for β- and γ2-subunits, respectively) suggests that this dual binding mechanism may have evolved as a mechanism to allow for a tight regulation of AP2 binding (and therefore internalization kinetics) by multiple signaling cascades that converge at the level of direct receptor phosphorylation. This mechanism would allow for the coordinated regulation via multiple separate signaling pathways of $GABA_AR$ cell-surface number by controlling the stoichiometry of β-subunit and/or γ-subunit phosphorylation and, subsequently, the kinetics of receptor endocytosis, with critical consequences on the efficacy of inhibitory synaptic transmission (28).

Materials and Methods

Antibodies and cDNA Constructs, Neuronal Culture, and Biotinylation Assays. Cultures and biotinylation of cortical neurons were performed as described previously (25). Antibodies to AP2 and $GABA_ARs$ and plasmids to the $GABA_AR$ subunit ICDs fused to GST, and the subunits of AP2 have been described previously (10, 13).

Detection of AP-2 μ-Chain Binding to $GABA_AR$ γ2-Subunit YECL Peptides by Affinity Pulldown and SPR Assays. SPR, affinity purification from rat brain lysate, [^{35}S]-labeled, or purified proteins with peptides linked to CH-Sepharose beads were performed essentially as described in a number of previous studies (see *SI Materials and Methods*) (10, 13, 31).

Crystallography of the μ2–AP2 $GABA_AR$ YECL-Pep Interaction. X-ray data for μ2 YECL-pep crystals was collected at PSF beamline BL2 of Freie Universitat Berlin at BESSY/Berlin and processed by using HKL2000 (32) and scalepack. The phase problem was solved by molecular replacement with CCP4 program molrep (33) by using Mu2 Adaptin Subunit (PDB ID code 1BW8) without water and ligand atoms as model (23). After rigid body refinement, the R value was 36.5% (R_{free} = 39.5%) for data between 40- and 3.0-Å resolution. Subsequent cycles of isotropic B value and positional refinement to 2.51-Å resolution were performed by using Refmac5 (34). The peptide chain and the missing residues were built manually by using the model-building program, Coot (for additional details, see *SI Materials and Methods*) (35).

Whole-Cell Recordings. Whole-cell recordings of mIPSCs from striatal neurons in acute slices used standard voltage-clamp techniques in the presence of 20 μM CNQX and 40 μM APV to block AMPA and NMDA receptors, respectively (see also *SI Materials and Methods*) (10, 25, 30).

ACKNOWLEDGMENTS. This work was supported by United Kingdom Medical Research Council funding (to J.T.K.) and Deutsche Forschungsgemeinschaft Grants SFB 449, TP A11, and Z3 (to W.S. and V.H.). S.J.M. is supported by National Institutes of Health grants NS046478, NS048045, NS051195, NS056359, P01NS054900, the Medical Research Council (UK), and the Wellcome Trust.

1. Kittler JT, McAinsh K, Moss SJ (2002) *Mol Neurobiol* 26:251–268.
2. Essrich C, Lorez M, Benson JA, Fritschy JM, Luscher B (1998) *Nat Neurosci* 1:563–571.
3. Crestani F, Lorez M, Baer K, Essrich C, Benke D, Laurent JP, Belzung C, Fritschy JM, Luscher B, Mohler H (1999) *Nat Neurosci* 2:833–839.
4. Moss SJ, Gorrie GH, Amato A, Smart TG (1995) *Nature* 377:344–348.
5. Brandon NJ, Delmas P, Hill J, Smart TG, Moss SJ (2001) *Neuropharmacology* 41:745–752.
6. Mielke JG, Wang YT (2005) *J Neurochem* 92:103–113.
7. Naylor DE, Liu H, Wasterlain CG (2005) *J Neurosci* 25:7724–7733.
8. McNamara JO, Huang YZ, Leonard AS (2006) *Sci STKE* 2006:re12.
9. Kittler JT, Delmas P, Jovanovic JN, Brown DA, Smart TG, Moss SJ (2000) *J Neurosci* 20:7972–7977.
10. Kittler JT, Chen G, Honing S, Bogdanov Y, McAinsh K, Arancibia-Carcamo IL, Jovanovic JN, Pangalos MN, Haucke V, Yan Z, Moss SJ (2005) *Proc Natl Acad Sci USA* 102:14871–14876.
11. Owen DJ, Collins BM, Evans PR (2004) *Annu Rev Cell Dev Biol* 20:153–191.
12. Bonifacino JS, Traub LM (2003) *Annu Rev Biochem* 72:395–447.
13. Haucke V, Wenk MR, Chapman ER, Farsad K, De Camilli P (2000) *EMBO J* 19:6011–6019.
14. Lee SH, Liu L, Wang YT, Sheng M (2002) *Neuron* 36:661–674.
15. Palmer CL, Lim W, Hastie PG, Toward M, Korolchuk VI, Burbidge SA, Banting G, Collingridge GL, Isaac JT, Henley JM (2005) *Neuron* 47:487–494.
16. Vissel B, Krupp JJ, Heinemann SF, Westbrook GL (2001) *Nat Neurosci* 4:587–596.
17. Kastning K, Kukhtina V, Kittler JT, Chen G, Pechstein A, Enders S, Lee SH, Sheng M, Yan Z, Haucke V (2007) *Proc Natl Acad Sci USA* 104:2991–2996.
18. Prybylowski K, Chang K, Sans N, Kan L, Vicini S, Wenthold RJ (2005) *Neuron* 47:845–857.
19. Roche KW, Standley S, McCallum J, Dune Ly C, Ehlers MD, Wenthold RJ (2001) *Nat Neurosci* 4:794–802.
20. Lavezzari G, McCallum J, Dewey CM, Roche KW (2004) *J Neurosci* 24:6383–6391.
21. Nesterov A, Carter RE, Sorkina T, Gill GN, Sorkin A (1999) *EMBO J* 18:2489–2499.
22. Honing S, Ricotta D, Krauss M, Spate K, Spolaore B, Motley A, Robinson M, Robinson C, Haucke V, Owen DJ (2005) *Mol Cell* 18:519–531.
23. Owen DJ, Evans PR (1998) *Science* 282:1327–1332.
24. Owen DJ, Setiadi H, Evans PR, McEver RP, Green SA (2001) *Traffic* 2:105–110.
25. Kittler JT, Thomas P, Tretter V, Bogdanov YD, Haucke V, Smart TG, Moss SJ (2004) *Proc Natl Acad Sci USA* 101:12736–12741.
26. Ricotta D, Conner SD, Schmid SL, von Figura K, Honing S (2002) *J Cell Biol* 156:791–795.
27. Nymann-Andersen J, Sawyer GW, Olsen RW (2002) *J Neurochem* 83:1164–1171.
28. Kittler JT, Moss SJ (2003) *Curr Opin Neurobiol* 13:341–347.
29. Schwartz-Bloom RD, Sah R (2001) *J Neurochem* 77:353–371.
30. Chen G, Kittler JT, Moss SJ, Yan Z (2006) *J Neurosci* 26:2513–2521.
31. Haucke V, De Camilli P (1999) *Science* 285:1268–1271.
32. Otwinowski Z, Minor W (1997) *Methods Enzymol* 276:307–326.
33. Project CC (1994) *Acta Crystallogr D* 50:760–763.
34. Murshudov GN, Vagin AA, Dodson EJ (1997) *Acta Crystallogr D* 53:240–255.
35. Emsley P, Cowtan K (2004) *Acta Crystallogr D* 60:2126–2132.